# INCUBATION TIME IN THE STRESS CORROSION CRACKING OF A LOW CARBON STEEL, A FRACTURE MECHANICS APPROACH USING THE J INTEGRAL PARAMETER

by

Adnan S.Koru

Submitted to the Faculty of Engineering
in Partial Fulfillment of
the Requirements for the Degree of
MASTER OF SCIENCE
in
MECHANICAL ENGINEERING



Boğaziçi University
1983

ACKNOWLEDGEMENTS

I am deeply indepted to my thesis adviser Doç.Dr. Öktem Vardar for his invaluable guidance and unceasing support without which the present work would not be possible at all. The realization of the experimental set-up was possible through the councel of Dr. Vahan Kalenderoğlu to whom I am similarly indebted.





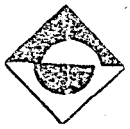

## ABSTRACT

The incubation period associated with the advance of a stress corrosion crack in a low carbon steel exposed to sulphuric acid is investigated. Fatigue pre-cracked Cantilever Beam Specimens are tested in accordance with Fracture Mechanics methodology.

Regarding the fact that the application of the Linear-Elastic-Stress-Intensity-Factor K to stress corrosion problems has met with extended success, the J Integral parameter with its broader scope of application is used in the same context. Considerable emphasis is placed upon establishing an effective and straightforward experimental method. Results obtained clearly indicate that the J Integral parameter is suitable for predicting incubation behaviour.

# ÖZET

Sülfürik asit ortamına tabi tutulmuş düşük karbon oranli çelik malzemede gerilmeli korozyon çatlağı oluşumundaki kuluçka zamani araştırıldı. Kırılma Mekaniği metodlarına uygun olarak bir çentik ve yorulma ön-çatlağı ihtiva eden Ankastre Numuneler kullanıldı.

Doğrusal Elastik Gerilme Şiddet Çarpanı K'nın gerilmeli korozyon problemlerine uygulanmasında elde edilen başarıların ışığı altında bu defa daha geniş uygulama imkanları içeren J-integrali parametresi aynı amaçla kullanıldı. Bilhassa etkili ve doğrudan sonuca yönelik bir deneysel yöntemin geliştirilmesine ağırlık verildi. J-integrali parametresinin kuluçka zamanı davranışını belirlediğini açıkça gösteren sonuçlar elde edildi.

TABLE OF CONTENTS

# CHAPTER I

## INTRODUCTION

Stress Corrosion is one of the various types of corrosion problems commonly encountered in the industrial utilisation of machine elements and structures. In order for stress corrosion to occur, two factors, stress and a harmful environment should coexist. In other words, distinct from other types of corrosion, the application of stress is a prerequisite for stress corrosion. The problem being once limited to a few special cases has become commonplace with the extended use of high strength materials in computer-aided designs incorporating higher levels of stress. Among others an illustrative example is the stress corrosion problems encountered in the landing gears of aircrafts in marine service.

The general progress of failure due to stress corrosion cracking is much similar to that of fatigue failure. The stressed material being subjected to its typical environment (not all corrosive environments cause stress corrosion failure in a typical material) develops stress corrosion cracks emanating from highly stressed regions on its surface. The stress raiser in question is commonly a notch or a machine mark or in other cases a crack which is previously introduced by other means. In the case of materials having perfectly smooth surfaces, corrosion pitting is responsable

for the initiation of cracks. In all cases the initiation of the stress corrosion crack takes up a definite period of time until the crack reaches a size that renders it detectable. This period of initiation is known as the incubation time and in general the degree of sophistication available in the method of crack detection is of secondary concern due to the fact that once the incubation period is over, the rate of advance of the stress corrosion crack is sufficiently high. From initiation on, the stress corrosion crack advances with a definite rate of advance provided that there is no relaxation of atress. Upon reaching a critical crack size, sudden and total failure sets in where the critical crack size is determined by mechanical parameters alone.

The classical approach to stress corrosion testing has constituted smooth specimens and the determination of total life values as a function of applied stress. It is observed that upon approaching applied stress values equalling yield stress, total life values tend to zero and at applied stress values less than a threshold value no stress corrosion failures are observed. However the smooth specimen approach has serious drawbacks [1]*.

---

* Numbers in square brackets indicate references, a list of which is provided at the end of the text.

One serious drawback of the "smooth specimen" approach is that it yields false indications of insusceptibility. Certain materials like Titanium alloys have immunity to pitting with the result that the material displays insusceptible behaviour in "smooth specimen" stress corrosion tests. On the other hand the same material initially provided with a notch or a crack may show striking susceptibility to stress corrosion cracking.

Another serious drawback is that the experimental results obtained in "smooth specimen" tests show considerable scatter such that statistical methods are often used in the quest for obtaining meaningful results. The inherent scatter in experimental data is due to the fact that a total life measurement in a "smooth specimen" test comprises the following scheme of events up to failure;

-Pitting on the surface of the specimen,

-The growth of the pit to sufficient depth such as to act as a stress raiser,

-The initiation of the stress corrosion crack,

-Growth of the stress corrosion crack,

-Failure upon the crack reaching a critical size.

As a final remark it should be stated that the results of "smooth specimen" tests do not predict the dras-

tically reduced life values in the case of specimens containing notches or pre-cracks. Predicting the behaviour of an existing crack is of utmost practical importance in order to determine the remaining safe life of a component in service.

From 1960's on, the introduction of Linear-Elastic-Fracture-Mechanics(LEFM) methodology has brought considerable insight into the formerly unpredicted failure behaviour of structures containing flaws in the form of notches or cracks. In contrast with the "smooth specimen" approach, LEFM methods aim at predicting the stress concentration behaviour in the viscinity of the existing crack-tip. More recently LEFM methodology has been shown to be applicable to an ever increasing scheme of material behaviour problems involving the presence of cracks, application to stress corrosion problems being one example.

However the Fracture Mechanics approach as stated in the above is not without its limitations. LEFM methodology being based upon the determination of the elastic stress field near the crack-tip is limited in its strict sense to the analysis of fully elastic problems.

Except for extremely brittle materials like glass the majority of engineering materials show varying

degrees of plastic behaviour concerning the vicinity of the crack-tip. In the case of relatively brittle materials displaying limited plastic behaviour, predictions of LEFM are applicable with the introduction of certain measures. However problems involving extended plasticity are beyond the scope of LEFM, tools of "elastic-plastic" fracture mechanics being applicable in such cases.

It should be noted that there are quite a few proposals regarding the analysis of elastic-plastic problems and as of today the argument is yet to settle in favor of one specific point of view. The J Integral parameter is one of the most powerful tools proposed for this purpose; its predictive capability and range of application is currently of considerable concern.

Regarding the fact that the application of LEFM methods to stress corrosion problems is similarly limited, the work presented herein aims at introducing the J Integral parameter to the analysis of stress corrosion problems in pursuit for a parallel enlargement in scope of application.

# CHAPTER II

## LINEAR-ELASTIC-FRACTURE-MECHANICS APPLICATIONS IN STRESS CORROSION CRACKING AND ITS LIMITATIONS

With the advent of Linear-Elastic-Fracture-Mechanics and with the introduction of the widely accepted Linear-Elastic-Stress-Intensity-Factor K, a breakthrough has been achieved in the analysis of the failure of structures incorporating cracks. The marked advantage of the LEFM approach in contrast to the "net-section stress approach" lies in the fact that the K parameter directly characterizes crack-tip conditions in terms of stress and strain singularities(See Appendix-A).

It was recognized that the behaviour of a stress corrosion crack could be analyzed by the use of the K parameter in view of the fact that the process is related to mechanical conditions at the tip of the stress corrosion crack. The initial attempts in this context have been provided by the well-known studies of Brown [2,3], the results indicating a well-defined relation between the applied K level and the total life of a pre-cracked specimen. It has also been asserted that for the specific material-environment pair in question, a threshold level of the linear-elastic-stress-intensity-factor(denoted $K_{ISCC}$) exists below which no extension

of the stress corrosion crack is observed.

Further work by Wei, Novak and Williams [4] has indicated that in addition to predicting total life values, the K parameter can be used to characterize different phases leading to failure. Incubation period; time required for the initiation of a stress corrosion crack from a pre-crack, life after initiation up to failure and the rate of advance of the stress corrosion crack have been shown to be clearly predicted in terms of the K value applied to the crack-bearing structure. The general appearance of typical results obtained are presented in figures 2-1 and 2-2 below. Results of repeated studies conducted by numerous experimenters clearly indicate that the K approach is generally applicable and as of today the K parameter is the single effective tool available for the purpose [5,6,7].

It should however be noted that the range of applicability of the K approach is limited by the very nature of the K parameter itself. K being a linear-elastic parameter looses its significance and its predictive power in the elastic-plastic regime where the size of the yield zone at the tip of the crack attains values comparable with other dimensions pertaining to the geometry in question. Experimental work regarding the applicability of the K parameter to stress

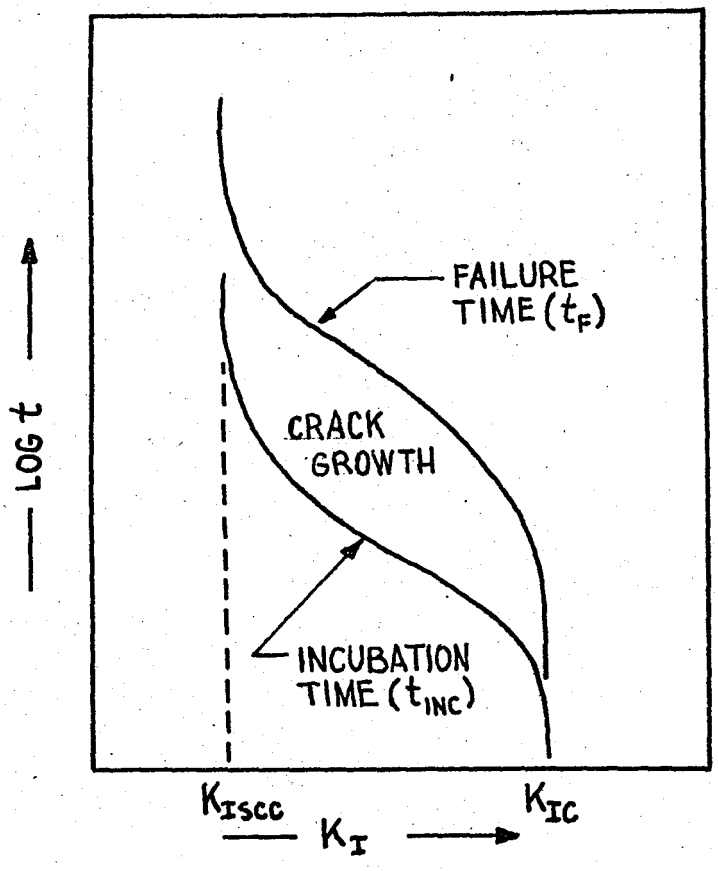


FIG. 2-1. Incubation and total life periods vs. applied K.

corrosion cracking have indicated that the parameter is inapplicable in cases where the above stated constraints are not fulfilled [1,4,5,8].

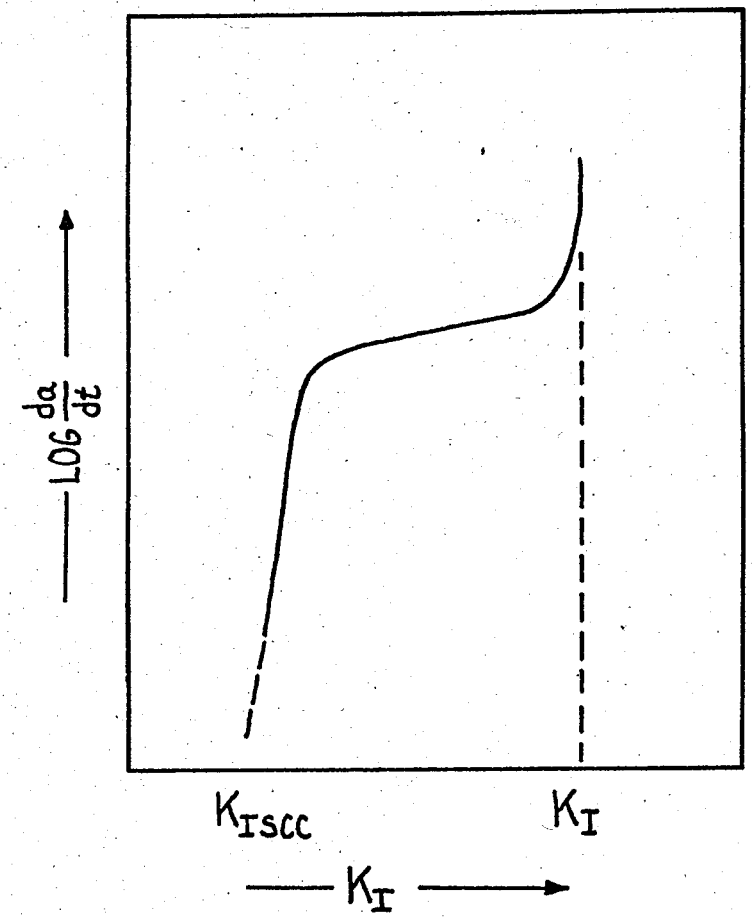


FIG. 2-2. Rate of advance of the stress corrosion crack vs. applied K.

# CHAPTER III

## THE J INTEGRAL PARAMETER

The J Integral has been introduced by Rice [9] as a path-independent energy line integral;

$$J=\int_{\Gamma}\left(Wdy - \vec{T}\cdot\frac{\partial\vec{u}}{\partial x}ds\right) \qquad (3\text{-}1)$$

where;

$\Gamma$-Any path around the crack-tip(See Fig. 3-1),

W-Strain-Energy density,

$$W=W(x,y)=W(\vec{\epsilon})=\sigma_{ij}d\epsilon_{ij}$$

and $\vec{\epsilon}=[\epsilon_{ij}]$, the infinitesimal strain tensor

$\vec{T}$-The traction vector defined according to the outward normal n along $\Gamma$,

$$T_i=\sigma_{ij}\,n_j$$

$\vec{u}$-Displacement vector,

ds-An element of arc length along $\Gamma$.

The path-independence of the J Integral as proved by Rice is valid for any linear-elastic or elastic-plastic material. The significance of the J Integral lies in the fact that it can be evaluated following any convenient path around the crack-tip and it can be used to characterize crack-tip conditions(e.g. in predicting fracture in the elastic-plastic regime).

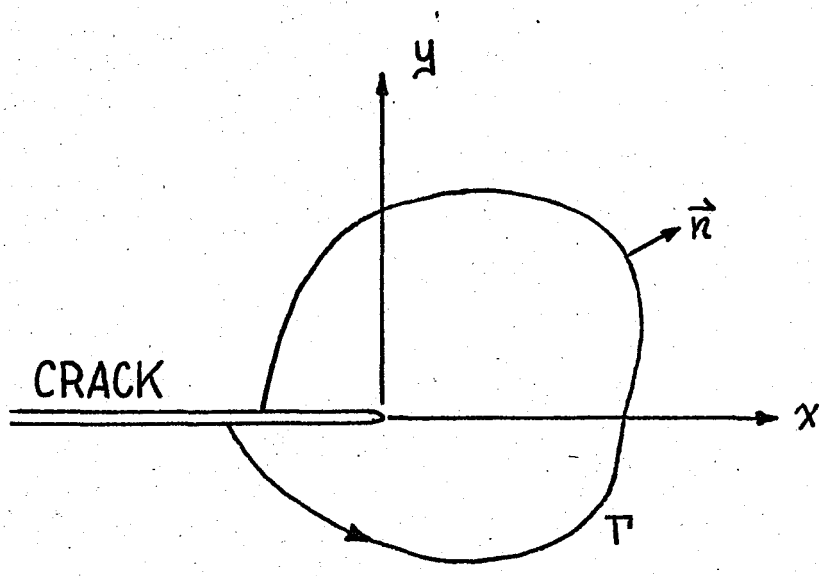


FIG. 3-1. Crack-tip coordinate system in two-dimensional deformation field and arbitrary line integral contour.

Parallelling the case where the K parameter does not loose significance despite a certain amount of crack-tip plastic yielding, the use of the J Integral can be extended to the case where a certain amount of large-scale yielding at the crack tip is admissible.

It has further been shown by Rice [9] that the J Integral may be interpreted as the potential energy difference between two identically loaded bodies having neighboring crack sizes;

$$J = -\frac{\partial P}{\partial l} \qquad (3\text{-}2)$$

where;

P-Potential energy per unit thickness,

l-Crack length.

Thus in the linear-elastic regime and for small-scale yielding, J is identical to G, the strain energy release rate parameter in the Griffith criterion of crack growth.

In the elastic-plastic regime the J Integral loses significance as the crack driving force(due to the irreversibility introduced by plastic yielding) but it is still effective in predicting fracture due to the fact that it characterizes crack-tip conditions [10] where a critical value of the J Integral, namely $J_C$ is used to predict elastic-plastic fracture.

J Integral value determination based on Eqt. 3-2 involves the use of a series of specimens with neighboring crack sizes. A simpler method using a single specimen has been introduced by Rice, Paris and Merkle [11] where the following expression is used to determine J Integral values*;

---

* Thus a single specimen is sufficient to determine the J value applied while in general a number of specimens is still required to determine the critical value of J for crack extension.

$$J = \frac{2A}{Bb} \qquad (3\text{-}3)$$

where;

A-The area under the load-load point displacement diagram,

B-Specimen thickness,

b-Length of the remaining ligament.

The method, intended for geometries where the remaining ligament is primarily subjected to bending (as in the Compact Tension and BEND type specimens) has been shown to be applicable by the work of Begley, Landes [12,13] and Hickerson [14].

# CHAPTER IV

# EXPERIMENTAL METHOD

## 4.1 Specimen Preparation

The configuration selected is the BEND type specimen (See Fig. 4-1) which is widely used in Fracture Mechanics testing. The BEND type specimen is normally intended for three or four-point bending while in this work the majority of specimens were subjected to cantilever loading hence the more appropriate name, "pre-cracked cantilever beam specimen".

The specimen dimensions are 14x14x100 mm., specimens being cut to length from 14 mm. square cold-drawn low carbon free-machining steel stock. The specimens are used in the as-received condition with no machining or heat treatment.

The chemical composition of the material based on manufacturer's specifications is given in table 4-1 below [15].

The mechanical properties of the material were determined by running a tensile test on an MTS Electro-Hydraulic Servo-Controlled Fatigue Testing Machine. The surface hardness of the cold-drawn stock was determined on a Rockwell Hardness Testing Machine. The results are summarized in table 4-2 below.

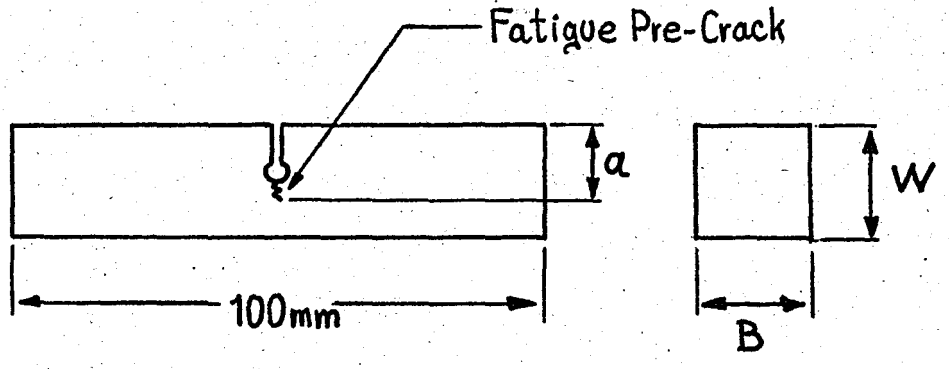


$W = 14$ mm

$B = 14$ mm

$a/W = 0.4 - 0.6$

FIG. 4-1. BEND type specimen.

TABLE 4-1. Chemical Composition of Low Carbon Cold-drawn, Free-machining Steel Used (in weight percent)

| C | Si | Mn | P | S |
|---|---|---|---|---|
| ≤0.14 | ≤0.05 | 0.9-1.3 | ≤0.1 | 0.24-0.32 |

TABLE 4-2. Mechanical Properties of Material Used

| | |
|---|---|
| Yield Strength ($S_y$) | - 64.0 kgf/mm$^2$ (91 ksi) |
| Tensile Strength ($S_u$) | - 68.9 kgf/mm$^2$ (98 ksi) |
| Hardness | - 55 $R_A$ |

On the specimen a notch of 1 mm. width is obtained by slitting to a pre-drilled hole of 2.5 mm. diameter. In view of Fracture Mechanics testing practice a fatigue pre-crack is introduced at the tip of the machined notch by cycling on the MTS Fatigue Testing Machine fitted with a three-point bending fixture. The initiation of the pre-crack has been facilitated and guided by deeply marking the notch-root using a sharp tipped knife. The total length "a" of the pre-crack and the machined notch has been kept to values yielding a/W ratios (See Fig. 4-1) between 0.4 and 0.6 .

An initial series of tests has clearly indicated that the maximum load value applied during fatigue cracking affects incubation behaviour. Excessive loading during pre-cracking induces undue plastic deformation at the crack-tip leading to an order of magnitude increase in incubation time values measured in stress corrosion tests that follow [16,17]. To obviate this effect the maximum load applied was kept below 400 kgf; the corresponding maximum value of linear-elastic-stress-intensity-

factor K thus attained is 88.9 kgf-mm$^{-3/2}$ (25.4 ksi$\sqrt{\text{inch}}$) .

## 4.2 Experimental Set-up

A cantilever loading fixture (See Fig. 4-2) , similar to that originally introduced by Brown [3], has been designed and constructed (an in scale drawing is available in Appendix C) . Due to its simplicity the fixture is widely used to conduct "total life" tests.

The specimen is fixed at one end to a rigid column which is attached to a rigid base. The other end is clamped

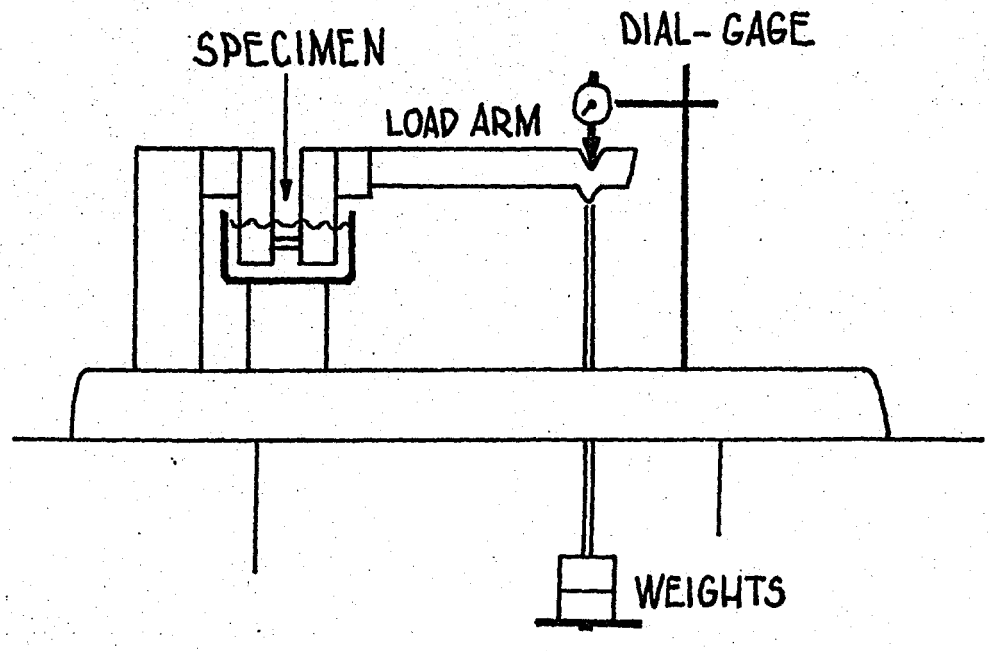


FIG. 4-2. Cantilever loading fixture.

to a loading arm of 46 cm. length. 40 mm. at each end of the specimen is used for clamping which leaves 20 mm. of the notch area exposed to the corrosive medium (See Fig. 4-3) . Two clamping caps are provided which are fixed by a total of eight bolts. Design details facilitate the alignment of the specimen.

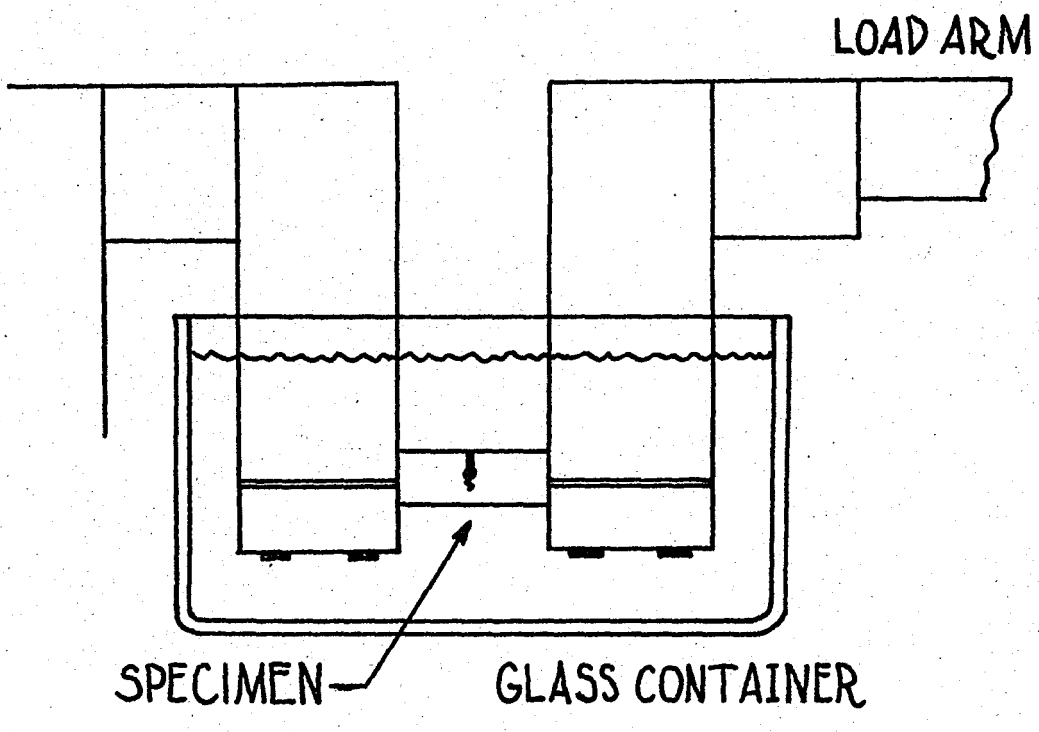


FIG. 4-3. Detailed sketch of the environment chamber.

As indicated in Fig. 4-3 above, the design of the fixture is unique in that a specially constructed environment chamber is not necessary. The corrosive medium is simply applied in a container of suitable shape. A glass container is actually used to facilitate the visual observation of the crack-tip region.

The corrosive medium used is 10 N $H_2SO_4$ solution. 400 $cm^3$ of solution is freshly prepared for each test; the volume being kept large to minimize the degradation of the solution during the course of the experiment. The solution is aerated by a stream of air bubbles supplied through plastic tubing and a small air-pump.

The specimen is loaded by adding 1/2 kg. weights to a weight-hanger attached by a knife-edge to the free end of the load arm. A dial-indicator supported by a stand on the base bears on the top end of the weight-hanger so that deflections on the load line can be measured directly. The dial-indicator has scale divisions down to 0.01 mm. and the measuring span of 20 mm. was observed to be more than adequate.

Originally a micro-switch had been attached to the extremity of the load arm to signal the initiation of the stress corrosion crack, but this was later removed due to the modification of the method used to detect crack initiation.

## 4.3 The Compliance Calibration Method

It is well-known that increasing the length of the crack in a typical specimen increases the mechanical compliance. Explicit expressions of elastic compliance for different specimen types are available in the literature [18].

Measuring compliance values was initially proposed as a means of detecting the initiation of the stress corrosion crack. The specimen with the fatigue pre-crack has a certain compliance which increases with the onset of stress corrosion crack growth. Initial tests have however indicated that while it is possible to detect crack initiation in this manner, a more practical and straightforward means was available (See Section 4.4). The method in turn was used to measure the initial length of the pre-crack.

Since the former intention was to conduct compliance measurements during the actual course of stress corrosion tests, a method was developed to yield compliance values directly on the loading fixture used.

A typical specimen displaying a certain amount of elastic-plastic behaviour yields a load-displacement plot as illustrated in Fig. 4-4 below. The record of load vs. displacement is in fact much similar to that obtained in a standard tensile test with an initial region of

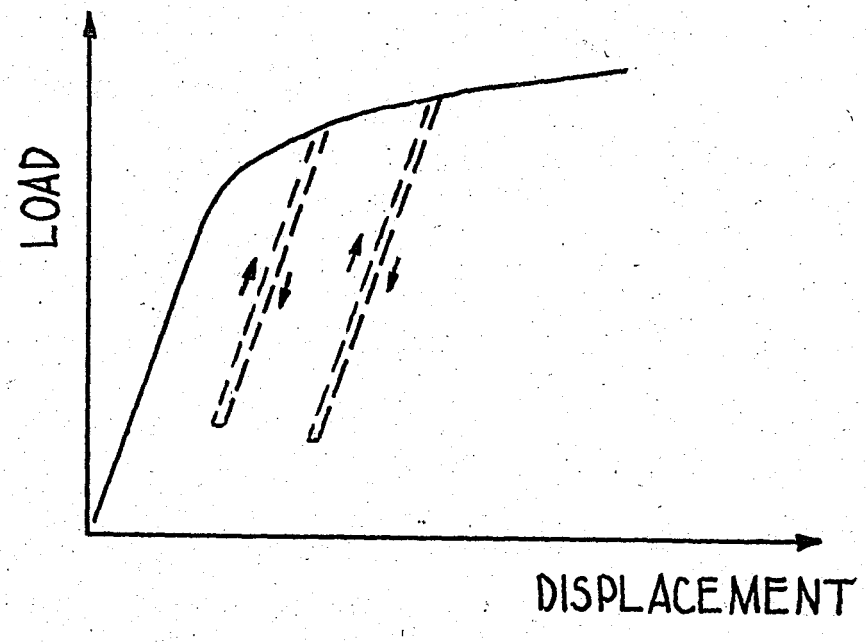


FIG. 4-4. Load-displacement behaviour of a typical specimen loaded well into the elastic-plastic region.

linear behaviour followed by non-linear behaviour upon approaching limit load.

It should be noted that the slope of the load-displacement plot at any point yields the inverse of the compliance value at that point. While the compliance value is unique in the linear region, this is not the case in the elastic-plastic region provided that comp-

liance is measured by additional forward loading. On the other hand unloading behaviour is constant throughout the elastic and elastic-plastic regions, hence measuring compliance by unloading is more instrumental in prescribing crack length. Determining the compliance behaviour of a crack-bearing specimen by unloading is known as the "unloading-compliance calibration method" [19,20].

The actual unloading-compliance calibration of the specimen mounted on the loading fixture was obtained by 17 fatigue pre-cracked specimens with a/W ratios ranging from 0.4 to 0.7 (See Fig. 4-5) . After the measurement of compliance the crack surfaces were left slightly ajar by introducing a wedge at the notch and the specimens were heat-tinted for about four hours in an oven at 250-300 °C . After cooling down to -10 °C to eliminate any plastic deformation, the crack surfaces were broken apart by applying an impact load of considerable magnitude.

The fracture surfaces were examined under a microscope of low magnification (30X) , the original crack area being easily identified by the dark color of heat-tinting. The crack area was estimated by taking measurements under the micraoscope with the aid of a 0.5 mm. grid. The area divided by the width of the specimen yields effective crack-length values(See Fig. 4-6) .

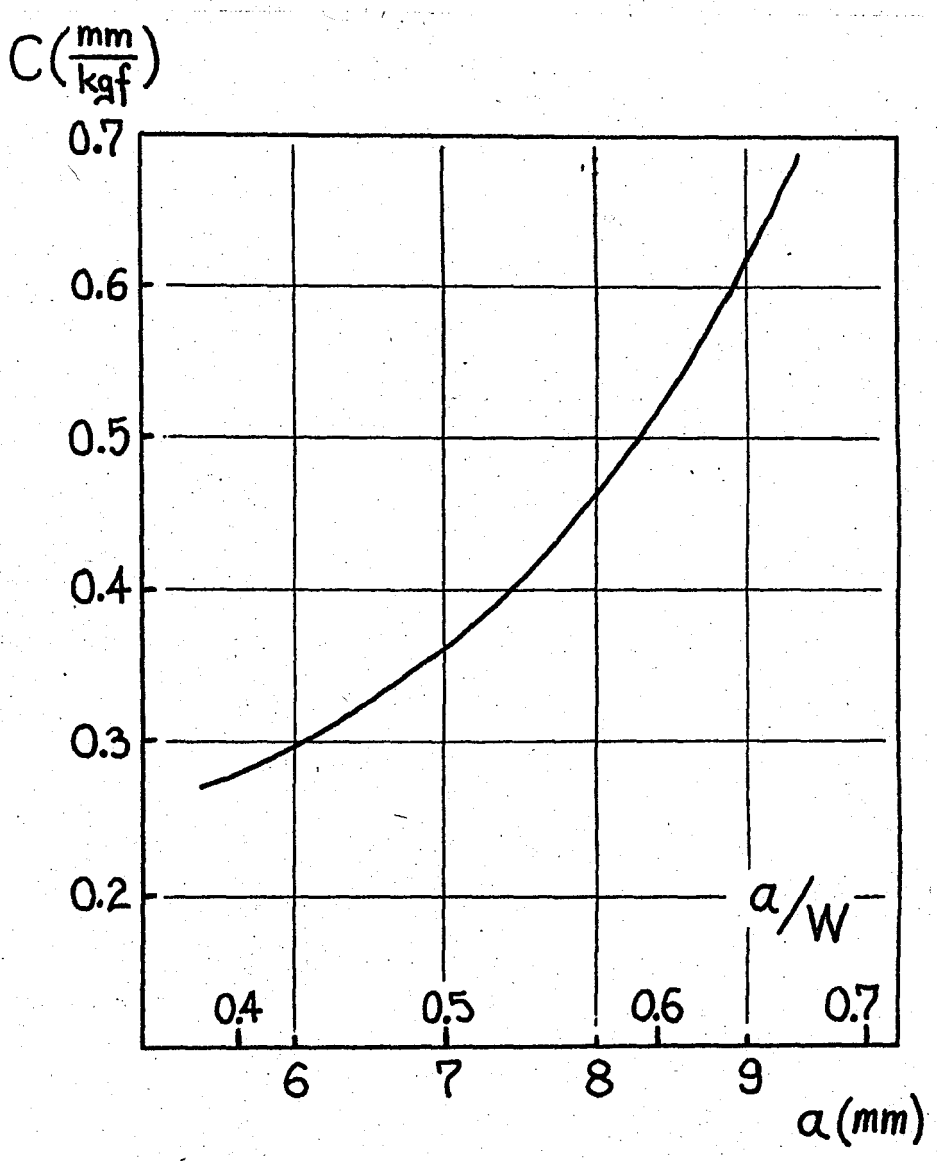


FIG. 4-5. The "unloading-compliance calibration" curve of the pre-cracked cantilever beam specimen.

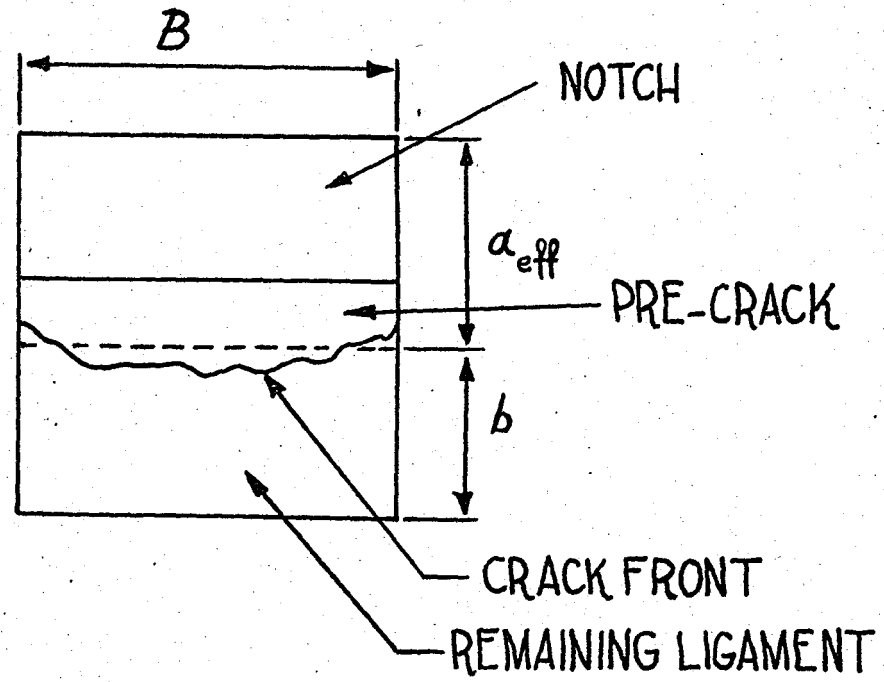


$$a_{eff} = \frac{\text{CRACK AREA}}{B}$$

FIG. 4-6. Estimation of effective crack-length.

Such a procedure for assessing crack-length values is instrumental due to the fact that the crack-front bows a considerable amount such that surface measurements on the two sides of the specimen are apt to yield underestimates.

## 4.4 Detecting the Initiation of Crack Growth

Detecting crack growth is in general limited by the accuracy of the available method for measuring crack-length. As noted in the previous section, the former proposal to detect the initiation of crack growth was to measure the change in the "unloading-compliance" value associated with crack advance. Although preliminary considerations have indicated that the accuracy involved is adequate for the purpose (detection down to 0.1 mm. crack advance being possible) , problems associated with the nature of the specific material-environment pair have been encountered.

During the course of actual experiments, corrosion by-products are formed at the tip of the pre-crack, the mechanical properties of these chamical species being such as to form a wedge which alters the unloading behaviour of the specimen (similar observations are reported by other investigators [21] ) . As a result the measured "unloading-compliance" values tend to increase considerably during the incubation period. A vague indication of crack advance is still possible due to the fact that compliance values eventually start to decrease and fall below the initial value. However the method is inprecise in terms of accurately detecting

crack initiation.

An alternate and more straightforward method is to observe directly the displacement behaviour of the specimen. The measurement of total elongation in smooth specimens has been used to monitor the growth of stress corrosion cracks [22] and crack opening displacement (COD) measurements in BEND type specimens have been used for the same purpose [23] .

Upon loading, the specimen shows a typical load-displacement behaviour and the maximum displacement value is preserved throughout the incubation period. With the initiation of the crack the loading-compliance of the specimen increases and the displacement value indicated by the dial-gage on the set-up displays a continually increasing behaviour. In cases where the specimen is loaded to values approaching limit load, a slight time-dependent increase in displacement is noted during the incubation period (See Fig. 4-7) , where the time dependence is related to extensive plastic yielding at the crack-tip. The displacement typically increases with a decreasing rate of increase. This behaviour is visually observed on the dial-indicator in the form of a slight creep which eventually dies out in a period of one to two minutes before the next increment of load is added. Increasing the load level accentuates this behaviour

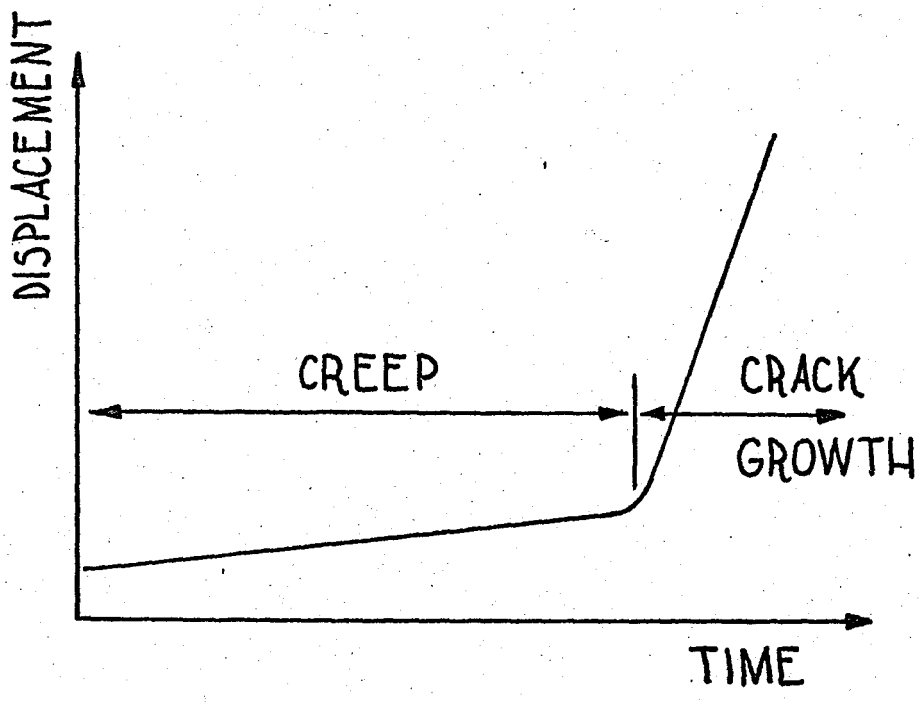


FIG. 4-7. Displacement behaviour of the specimen during the incubation period.

such that comparatively longer periods are necessary in order that the dial-indicator settles down to a stationary value. With the addition of the terminal weight a similar scheme of events take place and the slight creep extends into the incubation period with a negligibly small rate of increase of displacement value. Similar behaviour is reported by Hideya Okada et al. [23] who

have used COD measurements to detect crack initiation.

The above stated behaviour however does not introduce any ambiguity in terms of detecting the initiation of crack growth. The rate of increase of displacement associated with crack advance (crack growth rates are enhanced by higher values of loading) is an order of magnitude larger than the slight creep observed during the incubation period. At load values approaching limit load where creep is most noticable, crack advance due to stress corrosion may be so fast as to cause almost instantenous failure at the end of the incubation period.

It should further be noted that the creep behaviour stated above is not associated with crack-tip mechanochamical processes related with stress corrosion due to the fact that similar behaviour is observed with specimens loaded in air. A simple analysis based on the compliance of the specimen similarly rules out the possibility of a meaningful amount of subcritical crack advance.

A final note on the effectiveness of the method used to detect crack initiation is associated with the specific specimen type selected. The BEND type of specimen in contrast to other specimen types such as the "compact tension specimen" (CTS) has a reduced width such that a certain amount of crack extension results in a more

pronounced change in the a/W ratio further facilitating the detection of crack advance in terms of displacement or compliance measurements. The increase in crack length is also accompanied by a comparatively higher rate of increase of the crack-tip stress-intensity-factor resulting in high rates of crack advance. In effect, the period after initiation up to total failure is typically a fraction of the incubation time involved. At high values of loading the rate of crack advance after initiation is so large that the value of minimum detectable crack extension looses significance. With its upper range extending into hours, the incubation period is expressed in minutes and crack advance in a minute may be a few orders of magnitude larger than the minimum value of detectable crack advance. At lower values of loading, rate of crack advance after initiation is reduced considerably while the method is suitable to detect effectively the onset of crack growth.

In the interest of verifying the above deductions regarding the effectiveness of the method, a certain number of specimens have been unloaded right after the detection of crack advance. After washing and drying, the specimens have been broken apart and the crack surfaces examined. In support of the fore-going argument crack extension has been barely noticeable.

## 4.5 Experimental Procedure for Stress Corrosion Tests

An initial run of 5 specimens was used to develop the procedure outlined below;

1. The acid solution used as the corrosive medium is prepared.
2. The specimen is clamped to the loading fixture and the dial-indicator is attached to its proper position.
3. By means of the weight hanger attached to the load arm, 1/2 kg. weight are slowly added to a total of 3 kg.
4. Deflection at 3 kg. weight is noted.
5. With care as not to disturb the set-up, the specimen is unloaded to 2 kg. weight.
6. The resulting deflection is noted which yields the "unloading-compliance" value corresponding to 1 kg. unloading.
7. The specimen is completely unloaded.
8. The crack-length "a" is aobtained from the "compliance calibration plot" by using the "unloading-compliance" value determined in (6) . Crack-length "a" is used to determine the remaining ligament length "b" which is further used in J Integral determination.
9. The corrosive environment is applied by placing the glass container at its proper position beneath the specimen (it is reported that in general the order in which the corrosive environment and loading are applied is prone to affect test results, it is also noted that the application of the environment after loading is apt to yield erratic results [24] ) .
10. The aerator is switched-on.
11. The required loading is applied by adding 1/2 kg.

weights successively. After the addition of each weight the displacement value on the dial-indicator is noted and plotted on a displacement graph. At higher values of loading a slight creep on the dial-indicator accompanies the addition of each increment of load. A brief period of a minute or two is needed such that the dial-indicator settles down and the corresponding deflection value can be taken.

12. With the application of the terminal weight a timer for measuring the incubation period is started. A period of about 10 minutes is expended during which the specimen is loaded but this period is not included in the incubation period mainly based on the fact that at lower values of loading the damage induced at the crack-tip is negligible compared to that observed under maximum load.

13. The displacement behaviour under applied load is monitored at suitable time intervals and displacement values are plotted on a displacement versus time graph (See Section 4.4) .

14. With the detection of crack initiation in the manner described in section 4.4, the timer is stopped and the length of the incubation period is noted.

15. The specimen is completely unloaded and the corrosive medium is removed.

16. The specimen is washed under running water and dried.

17. The specimen is detached from the loading fixture and broken apart for further investigation of the crack surfaces.

## 4.6 Determination of J Integral Values

The expression (3-3) proposed by Rice, Paris and Merkle [11] is used for J Integral calculations. The dial-indicator on the loading fixture bears directly on the

weight hanger hence the deflection values are load-line deflections. In other words, the area under the resulting load-deflection plot yields the work done on the specimen during loading. Since the cantilever fixture and the load arm are specially designed to offer minimal flexure under load, the elastic deflections of the fixture itself is ignored. The load arm and the weight hanger being of considerable weight themselves contribute to the loading of the specimen. This contribution to the area under the load-displacement plot is accounted for by noting the position of the center of gravity of the load arm, the weight of the weight hanger, the length of the load arm and the initial loading compliance of each specimen.

The value of area A in expression (3-3) being thus determined, the length of the remaining ligament b is obtained by consulting the "compliance calibration curve". Further noting the thickness of the specimen B, the J Integral value corresponding to each loading is determined.

## 4.7 Results of Stress Corrosion Tests

After the establishment of the "unloading-compliance calibration curve" a total of 16 specimens have been subjected to stress corrosion tests. Specimen preparation and the details of the actual test are already presented in foregoing sections. The data thus obtained is presented in Table 4-3 .

TABLE 4-3. Results of Stress Corrosion Tests

| Specimen# | App. J (kgf/mm) | Incub. time (min.) | Max. load applied (kgf/mm) | a/W |
|---|---|---|---|---|
| 22 | 1.11 | 70 | 13.0 | 0.54 |
| 24 | 0.80 | 170 | 6.0 | 0.68 |
| 30 | 1.73 | 45 | 17.0 | 0.52 |
| 31 | 0.85 | 148 | 5.0 | 0.72 |
| 32 | 0.93 | 95 | 5.5 | 0.71 |
| 35 | 0.59 | 267 | 7.5 | 0.60 |
| 41 | 1.31 | 101 | 3.5 | 0.74 |
| 42 | 0.71 | 253 | 6.5 | 0.65 |
| 43 | 0.98 | 110 | 8.0 | 0.60 |
| 44 | 0.96 | 221 | 7.0 | 0.66 |
| 50 | 2.27 | 20 | 21.0 | 0.46 |
| 51 | 1.35 | 68 | 11.5 | 0.58 |
| 52 | 1.51 | 47 | 18.5 | 0.44 |
| 54 | 0.63 | 276 | 9.0 | 0.56 |
| 55 | 2.07 | 26 | 20.0 | 0.49 |
| 59 | 0.47 | 372 | 6.0 | 0.61 |

The loading of the specimens have been selected to cover a J Integral value range from 0.45 to 2.25 kgf/mm. The incubation periods observed range from 20 minutes to over 6 hours. The results are plotted on linear and semilogarithmic scales and presented in figures 4-8 and 4-9 below. A logarithmic plot is as well presented in figure 4-10 .

Although lower values of loading are within the scope of the linear-elastic-stress-intensity-factor K, higher values of loading involve considerable plastic yielding (indicated by large values of calculated plastic zone sizes) such that the applicability of K is out of question even from a practical point of view. The J Integral parameter is clearly applicable throughout the range considered. The low value of scatter in incubation period values indicate that the J Integral parameter is a good candidate to predict incubation behaviour in the elastic and elastic-plastic regime of loading. It should be noted that while the prime concern in the applicability of the J Integral involves the elastic-plastic regime, the parameter is fully applicable in the elastic regime as well.

The general trend of incubation behaviour is similar to that reported by other investigators on experimental studies concerning the application of the linear-elastic-stress-intensity-factor K [4,16] . Increasing values of

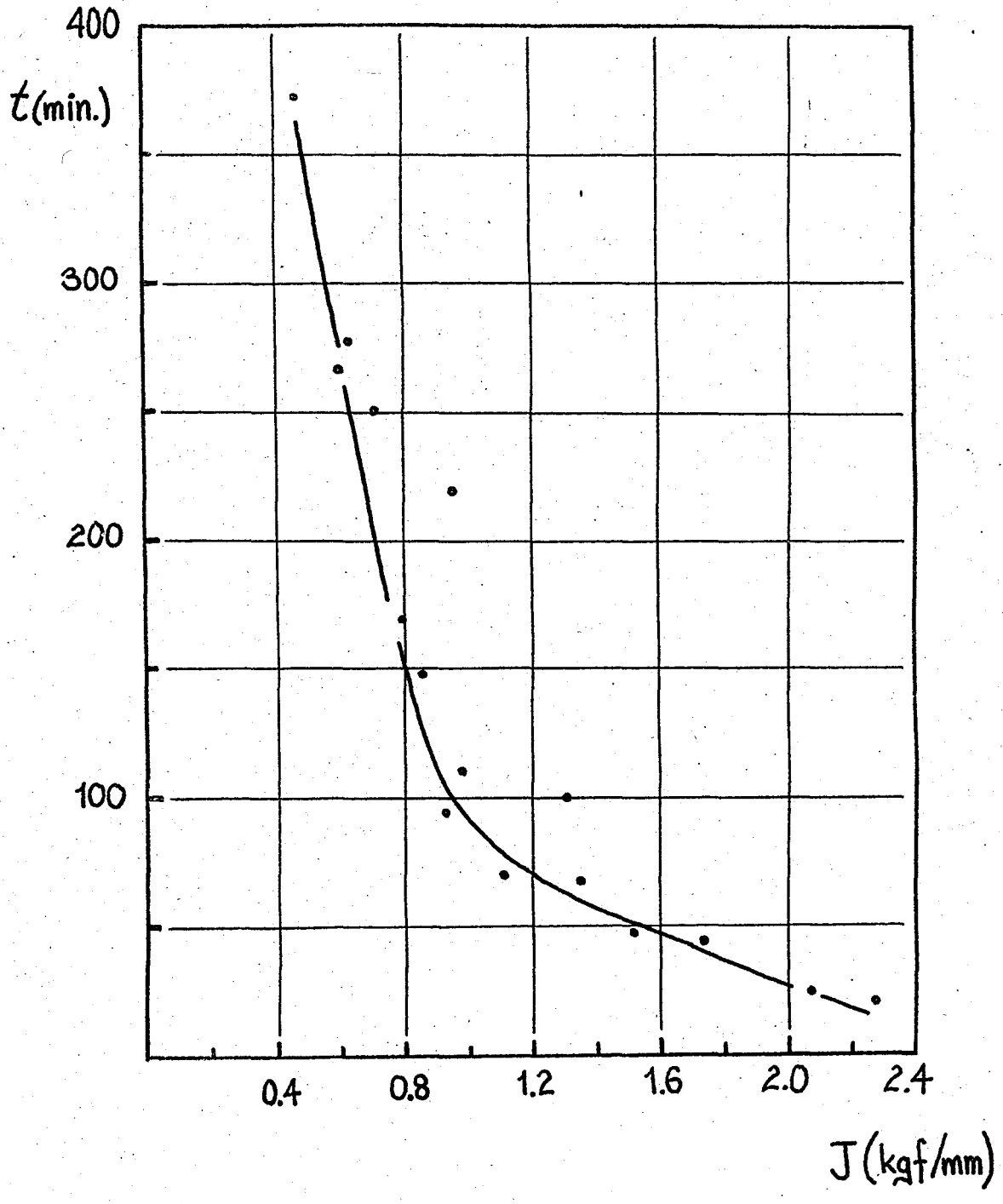


FIG. 4-8 Linear plot of incubation behaviour.

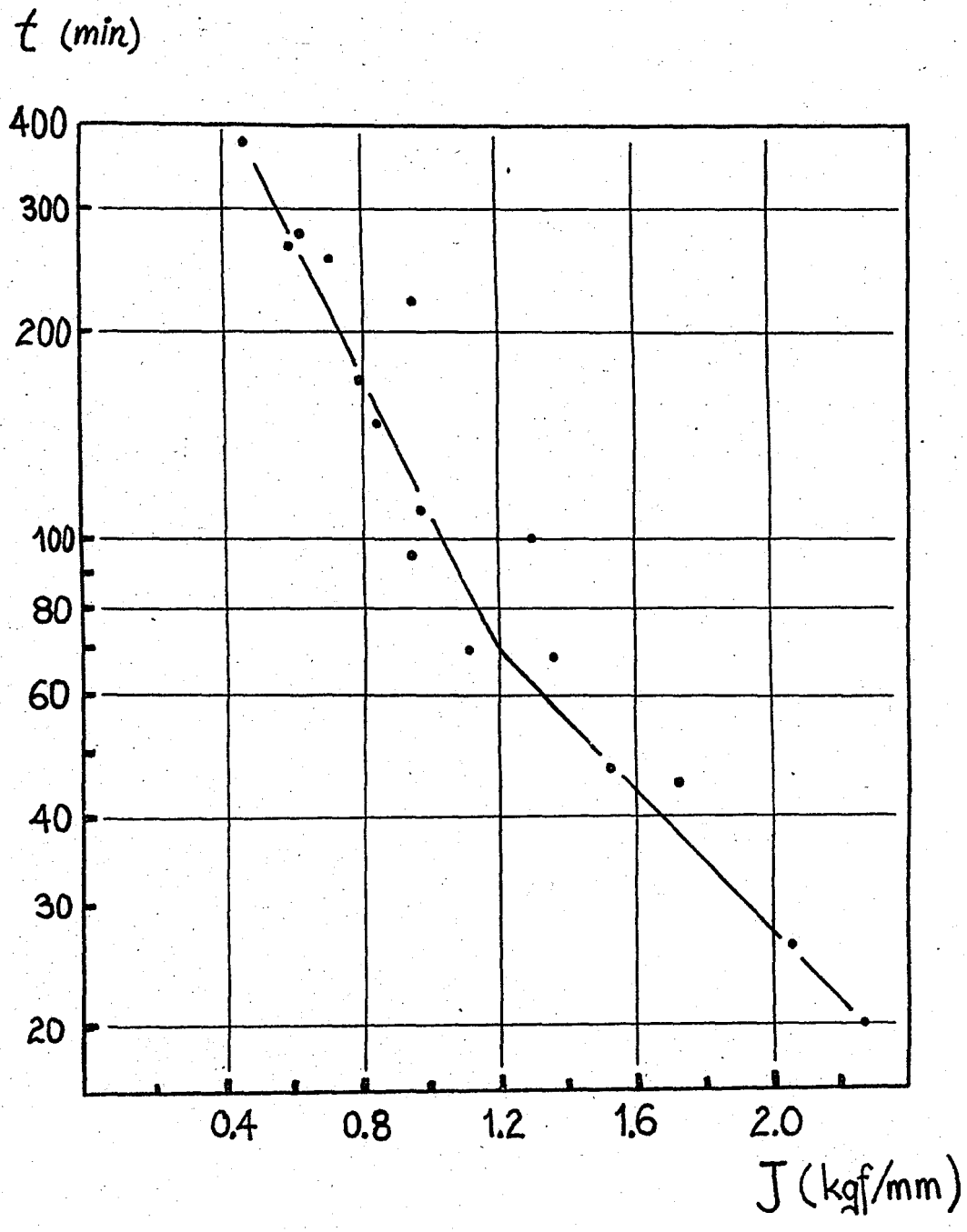


FIG. 4-9. Semilogarithmic plot of incubation behaviour.

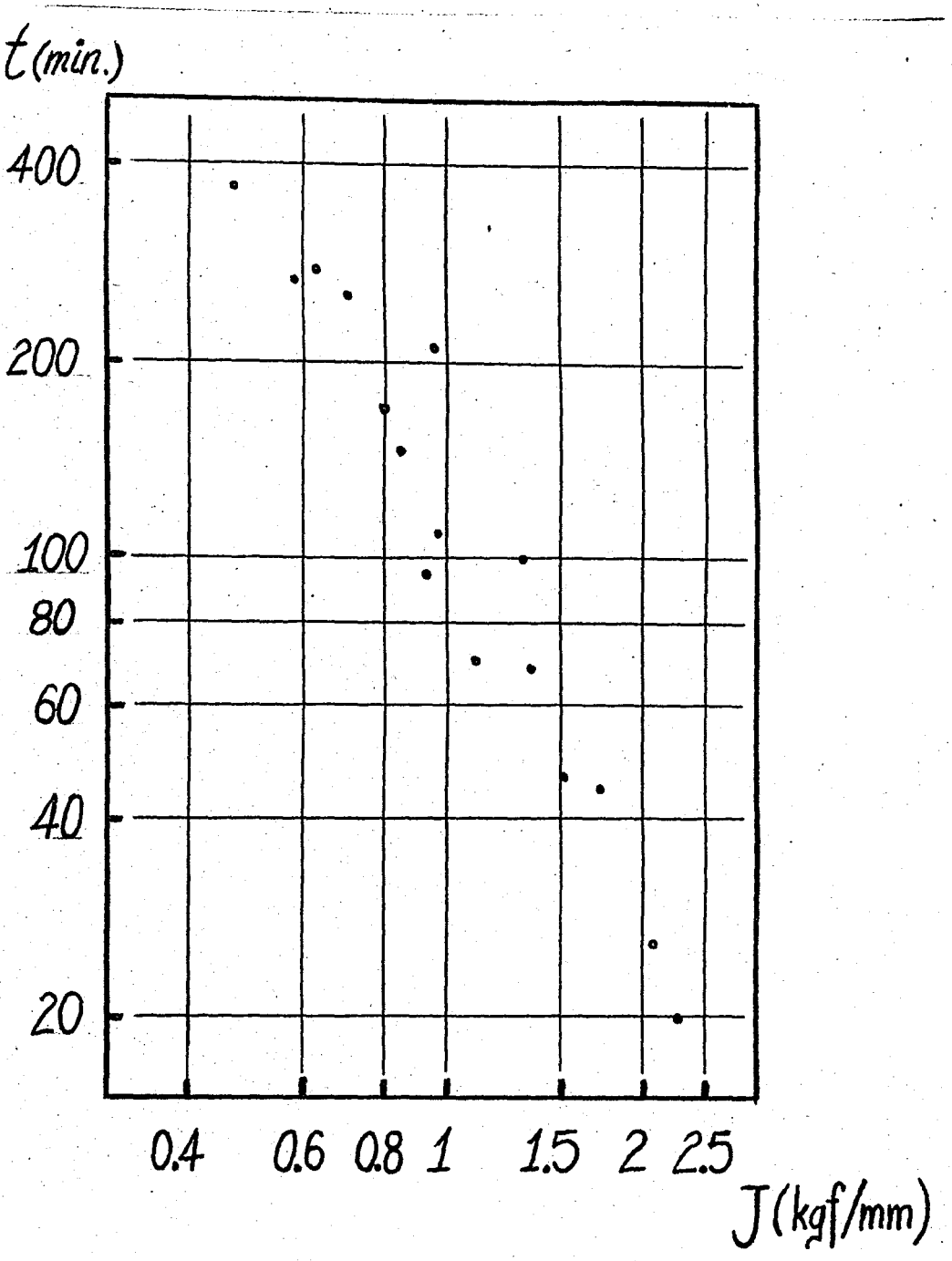


FIG. 4-10. Logarithmic plot of incubation behaviour.

applied J results in decreasing incubation period values which eventually tend to zero with the application of the critical value of J denoted by $J_{IC}$. Decreasing values of applied J on the other hand result in increasing incubation period values. The trend is such that no failure is expected below a threshold of 0.4 kgf/mm. which in turn can be considered as a tentative value for $J_{ISCC}$ (the threshold value of J analogous to $K_{ISCC}$ below which no stress corrosion crack is expected to initiate). However it should be noted that the determination of a true threshold value is beyond the scope of the present work in that, experimental studies in this regard involve tests running into well over 1000 hours [1,4] as well as the fact that the use of the linear-elastic parameter $K_{ISCC}$ for the purpose in question is well established.

## 4.8 $K_{IC}$ and $J_{IC}$ Tests

In order to determine the fracture toughness of the material used for stress corrosion tests, a $K_{IC}$ test has been carried out according to ASTM standards [25] . A BEND type specimen similar to those used for stress corrosion tests has been prepared and fitted with knife-edges to facilitate the attachment of a

standard clip-gage. The specimen has been statically loaded under displacement control on the MTS Fatigue Testing Machine. A three-point bending fixture has been used (See Fig. 4-11 below) . The crack opening displacement (COD) data from the clip-gage and load data from

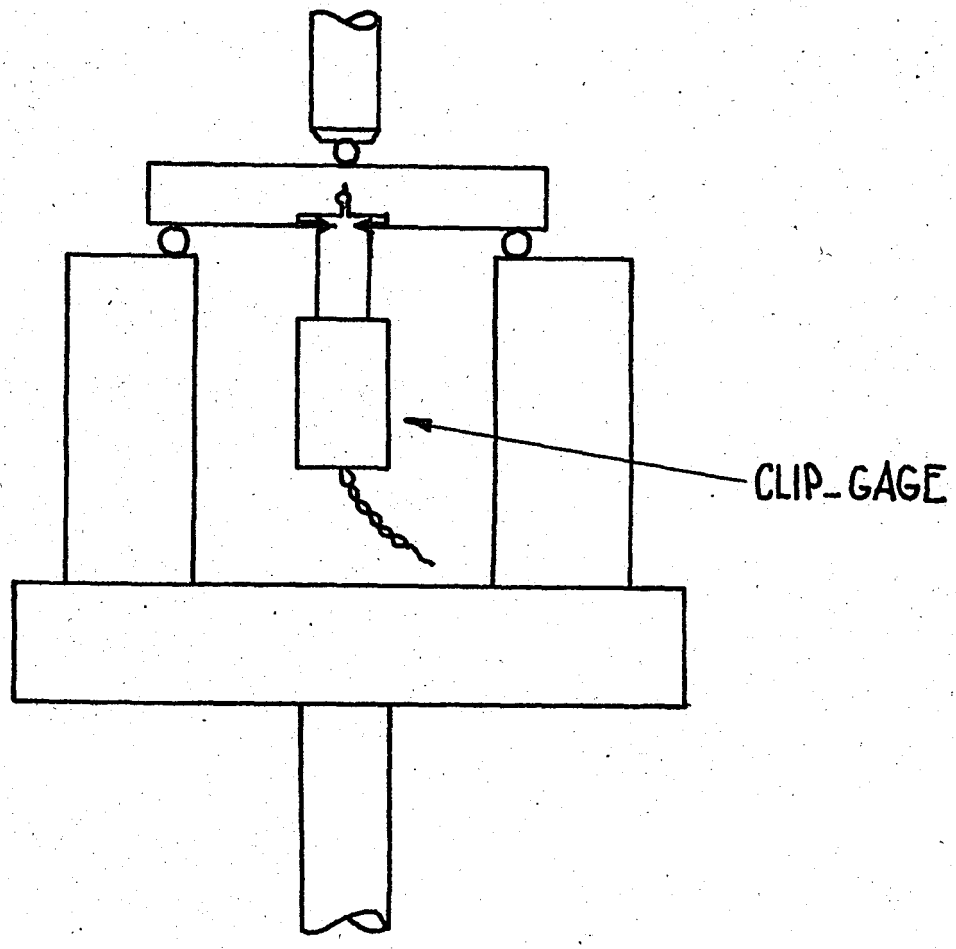


FIG. 4-11. Specimen configuration for $K_{IC}$ testing.

the load-cell provided on the MTS have been plotted on an X-Y plotter.

An analysis of the plot thus obtained yields a tentative fracture toughness value $K_Q$ of 122.5 kgf-mm$^{-3/2}$. (35 ksi$\sqrt{\text{inch}}$ ) . The load-COD plot however involves an unacceptable amount of non-linearity and minimum specimen size restrictions are not fulfilled indicating that the above stated tentative value can not be considered to be a true $K_{IC}$ fracture toughness value.

Three similarly prepared specimens (with no provision for clip-gage attachment) and the same three-point bending fixture have been used for $J_{IC}$ testing. The load-line displacement values have been measured by the linear variable differential transformer (LVDT) provided on the loading ram of the MTS. Together with load data from the load-cell on the machine, displacement controlled load-displacement graphs have been plotted on the X-Y plotter.

The actual load-displacement plot displays a well-defined peak in load value beyond which there is a sudden relaxation of load indicating crack advance. In order to detect possible subcritical crack advance before the attainment of peak load, two specimens have been carefully loaded just up to this peak value. The specimens have been heat-tinted and broken apart.

Inspection under the optical microscope (30X) has not revealed any crack extension hence the peak point has been selected as the point of crack extension. The area under the load-displacement plot up to this point of crack extension has been used as the basis for $J_{IC}$ calculation in accordance with equation (3-3) .

Due to the fact that the LVDT measures the deflection of the specimen as well as that of the loading fixture, a "compliance-correction" technique proposed by Server [26] has been used. The method involves a simple manipulation regarding the compliance of the fixture which is simply determined by substituting a large slab of steel in place of the specimen. The resulting $J_{IC}$ value has been determined as 2.38 kgf/mm.

# CHAPTER V

## CONCLUSIONS

A series of stress corrosion tests have been performed to analyze the applicability of the elastic-plastic fracture mechanics parameter J to predict incubation behaviour. The material properties and specimen configuration have been such that the larger portion of experimental work has been carried out under elastic-plastic conditions, constituting the primal area of application of the J Integral parameter. Conclusions obtained are summarized below.

1. The low level of scatter in experimental results clearly indicate that the J Integral parameter determined per the proposal of Mercle et al. [11] is a valid tool to prescribe incubation behaviour in a loading regime which is beyond the scope of of application of the linear-elastic-stress-intensity-factor K.

2. The general trend observed in incubation behaviour is similar to other published results based on experimental work employing the linear-elastic parameter K within its proper scheme of application.

3. For the specific material-environment pair in question (low carbon steel and sulphuric acid) a tentative threshold J Integral value $J_{ISCC}$ of 0.40 kgf/mm. is indicated while it should be noted that a more stringent testing procedure is necessary to determine a true threshold value. The corresponding $K_{ISCC}$ value calculated for plane-strain conditions is 94.3 kgf-mm$^{3/2}$ (27 ksi $\sqrt{\text{inch}}$ ) .

4. The BEND type specimen affixed to a cantilever loading fixture (pre-cracked cantilever beam specimen) has constituted an effective and practical method of testing for incubation behaviour. A simple consideration of the load-displacement behaviour of the specimen has formed a straightforward method for the detection of crack initiation. The method has obvious practical advantages over other proposed methods which include the visual observation of the crack area and more sophisticated methods which involve the use of ultrasonic waves and the method known as the "potential-drop calibration technique", all having respective shortcomings. It should further be noted that the "unloading-compliance calibration

method"has been ineffective in detecting crack growth due to the accumulation of corrosion by-products at the crack-tip. The method in turn has been used to measure initial values of crack length.

5. It has been observed that excessive loading during pre-cracking has a pronounced effect on incubation behaviour in the form of exaggerated incubation periods. To obviate the above effect, maximum loading during pre-cracking have been kept to a stress-intensity-factor value of 88.9 kgf-mm$^{-3/2}$ (25.4 ksi$\sqrt{\text{inch}}$ ) . Crack initiation during pre-cracking with the above restriction involves considerable work on the fatigue testing machine, number of cycles required runs into well over 100,000.cycles.

6. The use of a relatively high concentration (10N) of an aqueous solution of $H_2SO_4$ has resulted in manageable periods of incubation for the low carbon steel used. Time required for each experiment has been restricted to below 7 hours, with the practical advantage that direct supervision was possible and elaborate data acquisition equipment was not necessary.

## APPENDIX-A. LINEAR-ELASTIC-FRACTURE-MECHANICS [27,28]

The near-field solutions of the stress and displacement fields at the tip of a crack are due to Irwin. A through crack of length 2a with mathematically sharp tips in an infinite plate is considered (See Fig. A-1 below) . The plate is subjected to plane-strain condi-

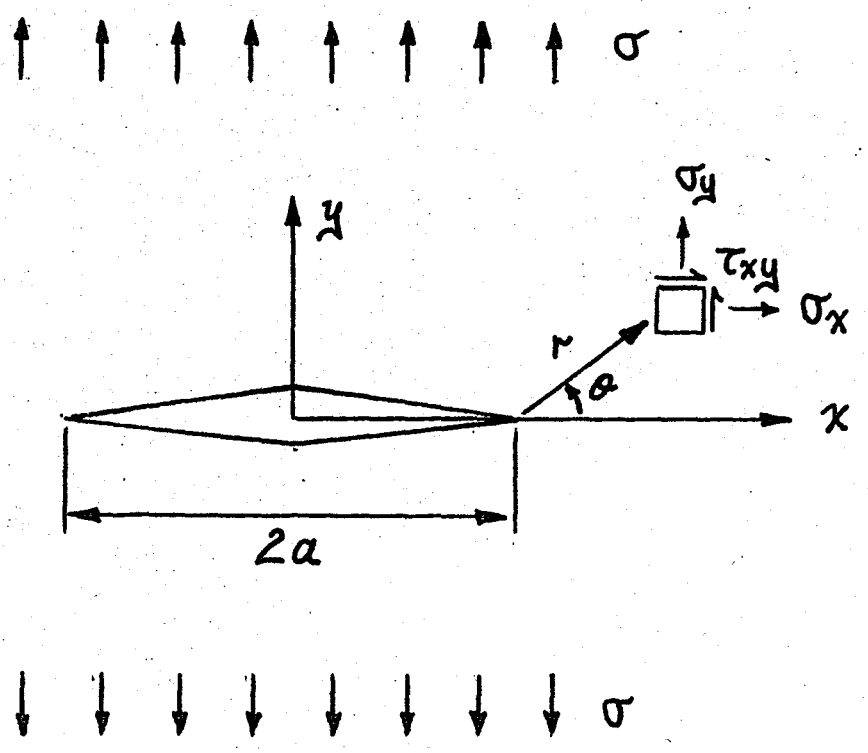


FIG. A-1. Crack in an infinite plate.

tions and the indicated form of loading is known as Mode I loading (hence the subscript in $K_I$) . The solution of the stress and displacement fields in familiar notation is given as;

$$\sigma_x = \frac{K_I}{\sqrt{2\pi r}} \cos\frac{\theta}{2}\left[1-\sin\frac{\theta}{2}\sin\frac{3\theta}{2}\right] \qquad \text{(A-1)}$$

$$\sigma_y = \frac{K_I}{\sqrt{2\pi r}} \cos\frac{\theta}{2}\left[1+\sin\frac{\theta}{2}\sin\frac{3\theta}{2}\right]$$

$$\tau_{xy} = \frac{K_I}{\sqrt{2\pi r}} \sin\frac{\theta}{2}\cos\frac{\theta}{2}\cos\frac{3\theta}{2}$$

$$\sigma_z = \nu(\sigma_x + \sigma_y)$$

$$\tau_{xz} = \tau_{yz} = 0$$

$$u = \frac{K_I}{G}\sqrt{\frac{r}{2\pi}} \cos\frac{\theta}{2}\left[1-2\nu+\sin^2\frac{\theta}{2}\right]$$

$$v = \frac{K_I}{G}\sqrt{\frac{r}{2\pi}} \sin\frac{\theta}{2}\left[2-2\nu-\cos^2\frac{\theta}{2}\right]$$

$$w = 0$$

where;

$\nu$-Poisson's ratio,

G-Shear modulus of elasticity,

u,v,w-Displacements respectively in the x, y and z-directions,

$K_I$ -Linear-elastic-stress-intensity-factor in mode I .

$$K_I = \sigma\sqrt{\pi a}$$

The stress field solutions expressing the initial terms of corresponding infinite series hold for the near-field where these terms dominate with $1/\sqrt{r}$ singularity. However an ideal material with infinite yield strength is considered while in an actual material of finite yield strength, a plastic zone of size $2r_y$ exists at the crack-tip. "$r_y$" is given by Irwin for plane strain as;

$$r_y = \frac{1}{6\pi}\left(\frac{K_I}{\sigma_{ys}}\right)^2 \qquad \text{(A-2)}$$

For cases where the plastic zone size is small (plane-strain conditions) in comparison with other dimensions of the geometry, the stress-field outside the plastic zone is still determined by the available expressions.

The linear-elastic-stress-intensity-factor K, incorporating the basic parameters $\sigma$ and a determine the intensity of the stress-field which is otherwise invariable. In this context K determines the onset of fracture in a specific material, the critical value being denoted by $K_{IC}$ .

The actual predictive power of the $K_{IC}$ parameter lies in the fact that for plane-strain conditions it is a material property irrespective of the geometry considered. In general for different geometries the K parameter can be expressed as;

$$K = \sigma c \sqrt{a} \qquad \text{(A-3)}$$

where c is defined as a function of geometric variables. Hence, once the $K_C$ value for a specific material is determined, fracture can be predicted irrespective of geometry provided that plane-strain conditions prevail and a K expression for the particular geometry is available.

As long as $r_y$ is less than 1/50 of the thickness in question, plane-strain conditions exist at the crack-tip. The condition for the applicability of the $K_{IC}$ parameter is given as;

$$B \geq 2.5 \left( \frac{K_{IC}}{\sigma_{ys}} \right)^2 \qquad \text{(A-4)}$$

At section sizes less than that expressed by the inequality (A-4) the $K_{IC}$ value increases with decreasing thickness. Plane-stress conditions being prevalent, the $K_{IC}$ parameter loses its theoretical and practical significance. Problems of such nature are the concern of elastic-plastic fracture mechanics.

## APPENDIX-B. K EXPRESSIONS FOR THE BEND SPECIMEN

For three-point bending [8];

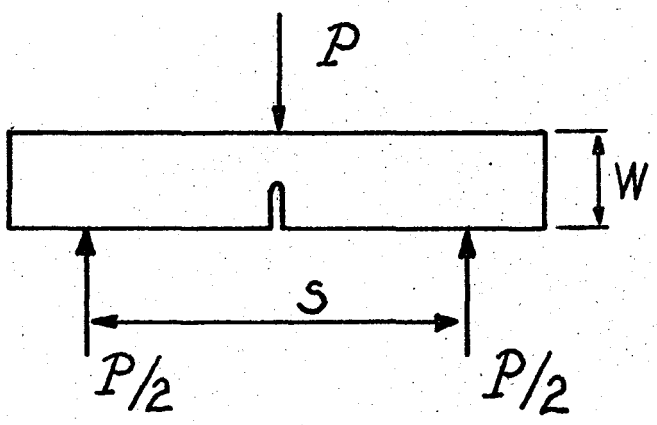


$$K_I = \frac{PS}{BW^{3/2}} \left[ 2.9\left(\frac{a}{W}\right)^{1/2} - 4.6\left(\frac{a}{W}\right)^{3/2} + 21.8\left(\frac{a}{W}\right)^{5/2} - 37.6\left(\frac{a}{W}\right)^{7/2} + 38.7\left(\frac{a}{W}\right)^{9/2} \right]$$

where;

P-Applied load,

B-Thickness of specimen,

S-Span,

W-Depth of specimen,

a-Crack length.

For cantilever loading;

While a manipulation regarding the bending moment applied at the crack surface is possible, a more straightforward expression is 3 ;

$$K_I = \frac{4.12\ m\ (\alpha^{-3} - \alpha^{3})^{1/2}}{B\ W^{3/2}}$$

where;

m-Bending moment at the crack surface,

B-Thickness of the specimen,

W-Depth of specimen,

$\alpha$- 1 - a/W

a-Crack length.

APPENDIX-C. IN SCALE DRAWING OF THE CANTILEVER LOADING FIXTURE

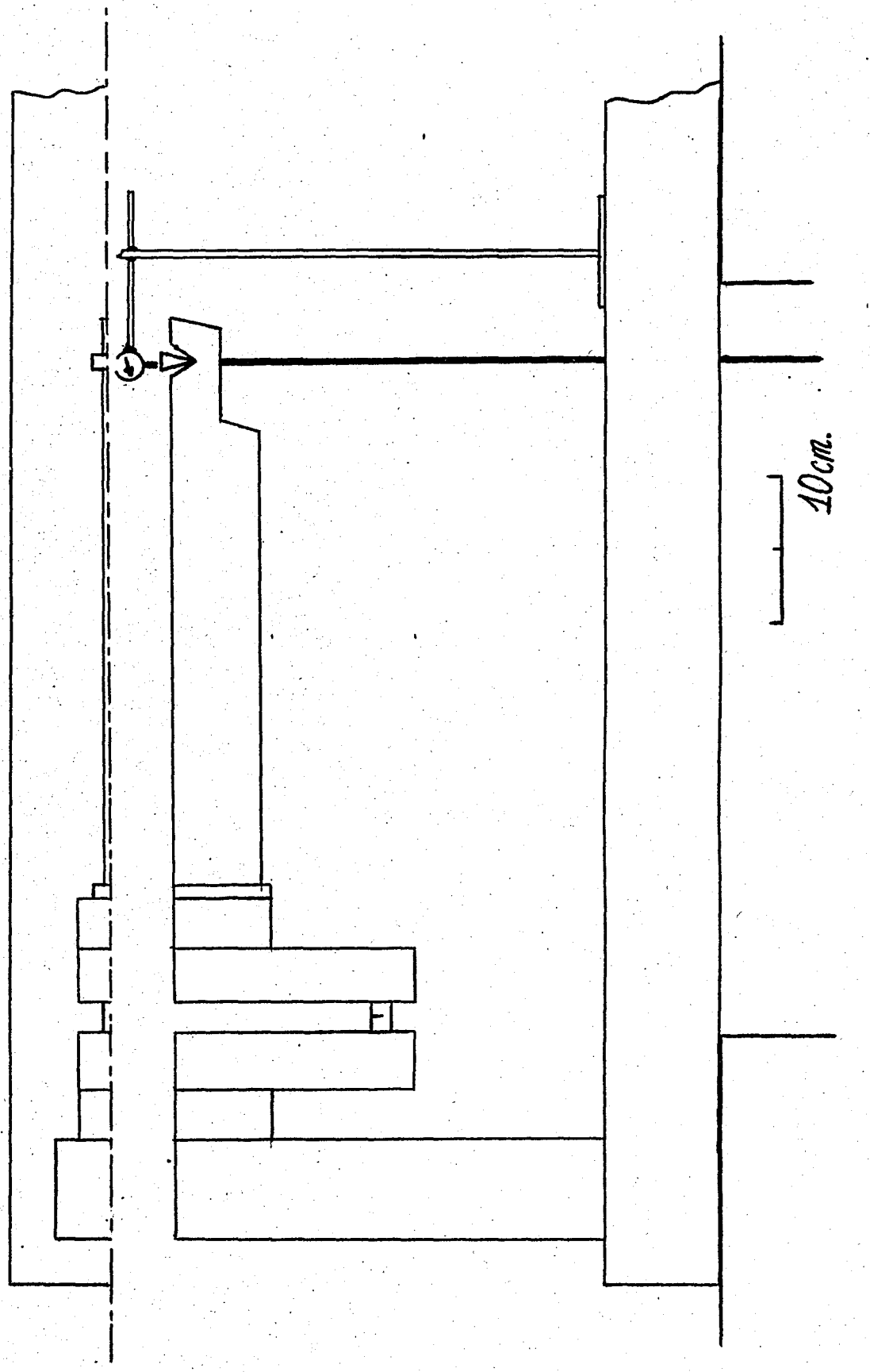

LIST OF FIGURES

## REFERENCES


1. Novak, S.R. and Rolfe, S.T., "Comparison of Fracture Mechanics and Nominal Stress Analyses in Stress Corrosion Cracking", Corrosion, Vol. 26, No. 4, April, 1970, pp. 121-130.

2. Brown, B.F. and Beachem, C.D., "A Study of the Stress Factor in Corrosion Cracking by Use of the Pre-cracked Cantilever Beam Specimen", Corrosion Science, Vol. 5, 1965, pp. 745-750.

3. Brown, B.F., "A New Stress Corrosion Cracking Test for High-Strength Alloys", Materials Research and Standards", Vol. 6, No. 3, March, 1966, pp. 129-133.

4. Wei, R.P., Novak, S.R. and Williams, D.P.. "Some Important Considerations in the Development of Stress Corrosion Cracking Test Methods", Materials Research and Standards, Vol. 12, No. 9, Sept. 1972, pp. 25-30.

5. Carter, C.S., "Application of Fracture Mechanics to Stress Corrosion Cracking", AGARD-AG-257, "Practical Applications of Fracture Mechanics", May, 1980.

6. Truman, J.E. and Haigh, P.M., "Basic Aspects of Stress Corrosion: The Role of Fracture Mechanics", Journal of the Institute of Metals, Vol. 101, 1973, pp. 221-224.

7. Judy, R.W., Jr. and Goode, R.J., "Stress Corrosion Cracking Characterization Procedures and Interpretations to Failure-Safe Use of Titanium Alloys", Transactions of the ASME, Journal of Basic Engineering, Vol. 91, No. 4, Dec. 1969, pp. 614-617.

8. Rolfe, S.T. and Barsom, J.M., "Fracture & Fatigue Control in Structures, Applications of Fracture Mechanics", Prentice-Hall, Inc., New Jersey, 1977.

9. Rice, J.R., "A Path Independent Integral and the Approximate Analysis of Strain Concentration by Notches and Cracks", Transactions of the ASME, Journal of Applied Mechanics, Vol. 35, No. 2, June, 1968, pp. 379-386.

10. Begley, J.A. and Landes, J.D., "The J Integral as a Failure Criterion", Scientific Paper 71-1E7-FMPWR-P3, Westinghouse Research Laboratories, Pittsburgh, 1971.

11. Rice, J.R., Paris, P.C., and Merkle, J.G., "Some Further Results of J Integral Analysis and Estimates", Progress in Flaw Growth and Fracture Toughness Testing, ASTM STP 536, 1973, pp. 231-245.

12. Landes, J.D. and Begley, J.A., "Test Results from J Integral Studies-An Attempt to Establish a $J_{IC}$ Testing Procedure", Scientific Paper 73-1E7-FMPWR-P3, Westinghouse Research Laboratories, Pittsburgh, 1976.

13. Landes, J.D. and Begley, J.A., "Recent Developments in $J_{IC}$ Testing", Scientific Paper 76-1E7-JINTF-P3, Westinghouse Laboratories, Pittsburgh, 1976.

14. Hickerson, J.P., Jr., "Comparison of Compliance and Estimation Procedures for Calculating J Integral Values", Flaw Growth and Fracture, ASTM STP 631, 1977, pp. 62-71.

15. "Stahlschlüssel", Verlag Stahlschlüssel Wegst K.G., Neckar/Germany-West.

16. Branco, C.M., Radon, J.C., and Culver, L.E., "Influence of Specimen Orientation and Loading History on S.C.C. In an Aluminum Alloy", Corrosion Science, Vol. 17, 1977, pp. 125-141.

17. Dull, D.L. and Raymond, L., "Stress History Effect on Incubation Time for Stress Corrosion Crack Growth in AISI 4340 Steel", Metallurgical Transactions, Vol. 3, Nov., 1972, pp. 2943-2947.

18. Srawley, J.E., International Journal of Fracture Mechanics, Vol. 12, No. 3, 1976, pp. 475-476.

19. Clarke, G.A., Andrews, W.R.. Paris, P.C. and Schmidt, D.W.. "Single Specimen Tests for $J_{IC}$ Determination", Mechanics of Crack Growth, ASTM STP 590, 1976, pp. 27-42.

20. Saxena, A. and Hudak, S.J., "Review and Extension of Compliance Information for Common Crack Growth Specimens", International Journal of Fracture, Vol. 14, No. 5, June, 1978, pp. 453-468.

21. Hyatt, M.V., "Use of Precracked Specimens in Stress Corrosion Testing of High Strength Aluminum Alloys", Corrosion, Vol. 26, No. 11, Nov. 1970, pp. 487-503.

22. Szklarska-Smialowska, Z. and Gust, J., "The Initiation of Stress Corrosion Cracks and Pits in Austenitic Cr-Ni Steel in $MgCl_2$ Solutions at 40-90 C", Corrosion Science, Vol. 19, 1979, pp. 753-766.

23. Hideya Okada, Ken-Ich Yukawa and Hideo Tamura, "Transition of Cracking Mechanisms from Active Path Corrosion to Hydrogen Embrittlement in High Strength Steels in Boiling Nitrate Solution", Corrosion, Vol. 32, No. 5, May, 1976, pp. 201-203.

24. Suss, H., "Practicality of Establishing Threshold Values to Eliminate Stress Corrosion Failures in Metals and Alloys", Corrosion, Vol. 17, No. 2, Feb. 1961, pp. 83-88.

25. "Standard Method of Test for Plane-Strain Fracture Toughness of Metallic Materials", ASTM Designation E 399-74, Part 10, ASTM Annual Standards.

26. Server, W.L., "Compliance Correction for Determining Load-Line Energies for Compact Fracture Toughness Specimens", Journal of Testing and Evaluation, Vol. 7, No. 1, Jan. 1979, pp. 29-32.

27. Broek, D., "Elementary Engineering Fracture Mechanics", Sijthoff and Nordhoff International Publishers, Alphen aan den Rijn, 1978.

28. Knott, J.F., "Fundamentals of Fracture Mechanics", Butterworth & Co (Publishers) Ltd, London, 1973.